21. Lillevang ST, Toft P, Nielsen B. A method for isolating granulocytes from rabbit blood without causing activation. *J Immunol Meth* 1994;169:137–138.
22. Böyum A, Lövhaug D, Tresland L, Nordlie EM. Seperation of leucocytes: improved cell purity by fine adjustments of gradient medium density and osmolality. *Scand J Immunol* 1991;34:697–712.
23. Peters AM, Roddie ME, Danpure HJ, et al. $^{99}Tc^{m}$-HMPAO labelled leucocytes: comparison with ^{111}In-tropolonate labelled granulocytes. *Nucl Med Commun* 1988;9: 449–463.
24. Allan RA, Sladen GE, Bassingham S, Lazarus C, Clarke SEM, Fogelman I. Comparison of simultaneous ^{99m}Tc-HMPAO and ^{111}In oxine labelled white cell scans in the assessment of inflammatory bowel disease. *Eur J Nucl Med* 1993;20:195–200.
25. Arndt J-W, van der Sluys-Veer A, Blok D, et al. Prospective comparative study of technetium-99m-WBCs and indium-111-granulocytes for the examination of patients with inflammatory bowel disease. *J Nucl Med* 1993;34:1052–1057.
26. Mansfield JC, Giaffer MH, Tindale WB, Holdsworth CD. Quantitative assessment of overall inflammatory bowel disease activity using labelled leucocytes: a direct comparison between indium-111 and technetium-99m HMPAO methods. *Gut* 1995; 37:679–683.
27. Oyen WJG, Boerman OC, van der Laken CJ, Claessens RAMJ, van deer Meer JWM, Corstens FHM. The uptake mechanisms of inflammation and infection localizing agents. *Eur J Nucl Med* 1996;23:459–465.
28. Hebbard GS, Salehi N, Gibson PR, Lichtenstein M, Andrews JT. $^{99}Tc^{m}$-labelled IgG scanning does not predict the distribution of intestinal inflammation in patients with inflammatory bowel disease. *Nucl Med Commun* 1992;13:336–341.
29. Arndt JW, van der Sluys-Veer A, Blok D, et al. A prospective comparison of Tc-99m-labeled polyclonal human immunoglobulin and In-111 granulocytes for localization of inflammatory bowel disease. *Acta Radiol* 1992;33:140–144.
30. Delgado Castro M, Lancha C, Prats E, et al. The diagnostic value of Tc-99m human polyclonal immunoglobulin imaging compared to Tc-99m HMPAO labeled leukocytes in inflammatory bowel disease. *Clin Nucl Med* 1997;1:17–20.

Distribution of Glutathione and Technetium-99m-*meso*-HMPAO in Normal and Diethyl Maleate-Treated Mouse Brain Mitochondria

Toru Sasaki, Yasuhisa Fujibayashi and Michio Senda

Positron Medical Center, Tokyo Metropolitan Institute of Gerontology, Tokyo; and Faculty of Pharmaceutical Sciences, Kyoto University, Kyoto, Japan

The aim of this study was to explain the contribution of mitochondria to the accumulation of ^{99m}Tc-*meso*-hexamethyl propyleneamine oxime (HMPAO) in the brain, after examinations were performed. **Methods:** We studied subcellular distribution of ^{99m}Tc-*meso*-HMPAO and glutathione (GSH) in normal and diethyl maleate (DEM)-administered mice. **Results:** In normal brain, major radioactivity was found in the mitochondrial (49.0%) and cytosolic fractions (33.0%), while the GSH content was high in the cytosol (63.2%) and mitochondria (30.6%). The radioactivity in mitochondrial, cytosolic, microsomal and nuclear fractions was decreased in a dose-dependent manner by DEM, a GSH depleting agent, to 32.2% (mitochondrial) and 24.7% (cytosolic) of the control by a dose of 550 mg/kg. The GSH content in mitochondrial and cytosolic fractions also decreased in a dose-dependent manner on DEM treatment to 29.3% (mitochondrial) and 30.0% (cytosolic) of the control by 550 mg/kg of DEM. A good correlation was found between the uptake of ^{99m}Tc-*meso*-HMPAO and GSH content in mitochondrial, cytosolic and nuclear fractions, with a correlation coefficient (r) of 0.814, 0.834 and 0.784, respectively. **Conclusion:** Mitochondria are a major subcellular fraction for the uptake of ^{99m}Tc-*meso*-HMPAO by the brain, and GSH in mitochondria contributes to the accumulation of ^{99m}Tc-*meso*-HMPAO.

Key Words: subcellular distribution; glutathione; mitochondria; technetium-99m-*meso*-hexamethyl propyleneamine oxime; brain

J Nucl Med 1998; 39:2178–2183

Technetium-99m-*d,l*-hexamethyl propyleneamine oxime (HMPAO) has been used widely as a blood flow imaging agent for the brain. In our previous study (*1*), we found that the uptake of *meso*-isomer of ^{99m}Tc-HMPAO was decreased in diethyl maleate (DEM, a glutathione depletor that acts through glutathione S-transferase)-treated mouse brain accompanying a decrease in glutathione (GSH) content, but that ^{99m}Tc-*d,l*-HMPAO uptake was not affected by the same treatment. In another experiment (*2*), we found similar observations in DEM-treated rat brain and buthionine sulfoximine (BSO, a GSH depletor that acts through γ-glutamylcysteine)-treated mouse brain. Based on these observations, we suggested the *meso*-isomer of ^{99m}Tc-HMPAO be used as a GSH imaging agent for the brain.

The exact mechanism of the retention of ^{99m}Tc-HMPAO, either *d,l*- or *meso*-, has not been clarified, although the following is proposed. As a lipophilic compound, ^{99m}Tc-HMPAO diffuses across the blood-brain barrier and is rapidly converted to a hydrophilic form retainable within the brain tissue. GSH is supposed to be responsible for the hydrophilic conversion and for the retention of ^{99m}Tc-HMPAO in the brain (*3,4*). We found that ^{99m}Tc-HMPAO showed reactivity not only to GSH but also to other molecules possessing a −SH group, such as GSH analog (Gly-Cys-Glu) and cysteine. However, ^{99m}Tc-HMPAO did not react with oxidized GSH or ascorbic acid. In a previous study (*2*), we determined the thiols in the nonprotein and protein-fractions of DEM-treated mouse and indicated that the nonprotein thiols were responsible for the retention of ^{99m}Tc-HMPAO in the brain. GSH accounted for almost all of nonprotein thiols in the brain. Another experiment in mouse brain homogenates indicated that GSH is a major contributor to the retention of ^{99m}Tc-HMPAO in the brain (*2*).

The rate of conversion of ^{99m}Tc-*d,l*-HMPAO to hydrophilic complex by GSH was much higher than that of ^{99m}Tc-*meso*-HMPAO: the same rate is achieved at only 1/37 the GSH concentration (*2*). Therefore, the kinetics of ^{99m}Tc-*d,l*-HMPAO are virtually unaffected by the GSH content, while uptake is determined mainly by blood flow. On the other hand, the conversion of ^{99m}Tc-*meso*-HMPAO to the retainable form by GSH is slower than the washout of the diffusible form from brain to blood. Accordingly, the uptake of *meso*-isomer reflects GSH content more than does blood flow.

In an in vitro study, Fujibayashi et al. (*5*) demonstrated that the conversion of ^{99m}Tc-*d,l*-HMPAO to hydrophilic complex in brain homogenates was enhanced when mitochondiral mem-

Received Mar. 2, 1998; accepted Apr. 12, 1998.

For correspondence or reprints contact: Toru Sasaki, PhD, Positron Medical Center, Tokyo Metropolitan Institute of Gerontology, 1-1 Naka-cho, Itabasahi, Tokyo 173, Japan.

brane was destroyed by heat treatment or detergents. They speculated that an unidentified factor, which has a −SH and is not an enzyme, contributes to that reaction. Since mitochondria do not synthesize GSH de novo (*6*), GSH is supplied from the cytosol by a mitochondrial GSH transport system (*6,7*). Recently, the mitochondrial GSH transporter was identified as different from sinusoidal or canalicular GSH transporters (*7*). The GSH concentration in mitochondria is maintained at a higher level than that in cytosol by this transport system (*8,9*). These findings led to our interest in the relation between the GSH content and in vivo uptake of ^{99m}Tc-*meso*-HMPAO in the mitochondrial versus the cytosolic fraction of the brain.

In this study, the subcellular distribution of ^{99m}Tc-*meso*-HMPAO and GSH in normal and DEM-administered mice was studied to investigate the retention of ^{99m}Tc-*meso*-HMPAO in the brain and the reduction in radioactivity uptake on DEM-treatment. Moreover, ^{99m}Tc-*meso*-HMPAO as a novel tool for assessing the GSH content in mitochondria and cytoplasm of the brain is discussed.

MATERIALS AND METHODS

Labeling of Technetium-*meso*- and *d,l*-HMPAO

Labeling of ^{99m}Tc-*meso*- and *d,l*-HMPAO was performed as described (*1*). The radiochemical purity checked by three different chromatographic systems (*2*) was >94% for ^{99m}Tc-*meso*-HMPAO and >90% for [^{99m}Tc] *d,l*-HMPAO, respectively.

Treatment of Animals and Injection of Technetium-99m-HMPAO

DEM (Wako Pure Chemical Industries, Ltd., Osaka, Japan) was dissolved in corn oil and injected intraperitoneally into ddY mice weighing about 30 g at a dose of 137.5 (a group of four mice), 275 (another group of four mice) and 550 mg/kg body weight (a third group of five mice). A group of five control animals were injected with corn oil only. One hour after the DEM treatment, 1.85 MBq of ^{99m}Tc-*meso*- or *d,l*-HMPAO was injected intravenously into the mouse. Thirty minutes after the tracer injection, the animals were killed and the forebrains were removed quickly and prepared as follows.

Preparation of Subcellular Fractions from Mouse Brain

Preparation of subcellular fractions from ddY mouse brain followed the method of De Robertis et al. (*10*). Forebrains were homogenized in 9 volumes of 0.32 *M*-sucrose using a Potter homogenizer. The homogenate was centrifuged at 900 g for 10 min (Kubota 7800; Kubota Seisa Kusho Co. Ltd., Tokyo, Japan). The sediment was washed twice and rehomogenized rapidly in 0.32 *M*-sucrose and centrifuged at 900 g for 10 min. This sediment was considered the nuclear fraction. The pooled supernatant was centrifuged at 11,500 g for 20 min (Kubota 7800). This sediment was rehomogenized in 0.32 *M*-sucrose and centrifuged at 11,500 g for 20 min. The sediment was considered the mitochondrial fraction. The pooled supernatant was centrifuged at 100,000 g for 30 min (Beckman TL-100 by ultracentrifuge; Beckman Japan Co. Ltd., Tokyo, Japan). The resulting sediment and supernatant fluid corresponded to the microsomal and cytosolic fractions, respectively.

Each subcellular fraction was subdivided into three portions for measurement of radioactivity, determination of GSH content and enzyme assay. The radioactivity in the subcellular fractions was measured by an auto-well scintillation counter (Aloka Co. Ltd., Tokyo, Japan).

Determination of Glutathione and Enzyme Assay in Subcellular Fractions

The GSH content was measured as described previously (*2*) using the high-performance liquid chromatographic electrochemical detection method with a glassy carbon electrode at 1.1V (cation-exchange column; Shodex SP-825; Shoko Co. Ltd., Tokyo, Japan; 8 mm I. D. × 75 mm; elution with 10 m*M* citric acid and 10 m*M* disodium hydrogen phosphate solution adjusted to pH2.1 with metaphosphoric acid; at the flow rate of 1 ml/min). Lactate dehydrogenase was determined by the method described by Sims et al. (*11*). Cytochrome *c* oxidase was determined by the method described by Dunkley et al. (*12*). Protein content was determined by the method of Lowry et al. (*13*) using bovine serum albumin (Sigma Chemical Co. Ltd., Tokyo, Japan) as standard. Enzymatic activity was expressed as μmol/mg of protein/min.

The ^{99m}Tc-*meso*-HMPAO radioactivity and GSH content were also expressed as a concentration assuming the water content of the mitochondrial matrix and cytoplasm to be 0.8 and 3.8 μl/mg protein, respectively (*8,14*).

Release of Technetium-99m Radioactivity, Glutathione and Marker Enzyme from Mitochondrial Fraction by Membrane Solubilizers

Each of 10 ddY mice was injected with 1.85 MBq of ^{99m}Tc-*meso*-HMPAO according to the procedure described above. The mitochondrial fraction was isolated as described above. Treatment of the mitochondrial fraction was by modification of methods described elsewhere (*15–17*). The pooled mitochondrial fraction was subdivided into three portions and was treated with membrane solubilizer: no treatment, digitonin that destroys cell membrane, or Triton X-100 (Wako Pure Chemical Industries, Ltd., Osaka, Japan) with sonication that destroys mitochondrial membrane. Each treatment was done in quadruplicate. The mitochondrial fraction was incubated with digitonin (Wako Pure Chemical Industries, Ltd.) (0.5 mg/ml) or Triton X-100 (Wako Pure Chemical Industries, Ltd.) (0.1%, V/V) in 2.5 m*M* ethylenediamine-tetraacetic acid, 17 m*M* 3-morpholinopropanesulfonic acid (pH7.4) for 2 min at room temperature. After the treatment with Triton X-100, this mitochondrial fraction was sonicated by a bath-type sonicator (US-10; Sakura Seiki Co. Ltd., Tokyo, Japan) for 5 min. The fraction treated with digitonin or Triton X-100 with sonication was then centrifuged at 13,000*g* for 3 min. The sediment of this and the nontreated mitochondrial fraction as a control were subdivided into samples for measurement of radioactivity, determination of GSH and enzyme assay of citrate synthase. Citrate synthase was determined as described by Srere (*18*). The enzymatic activity was expressed as μmol CoASH formation/min.

RESULTS

Subcellular Distribution of Technetium-99m-HMPAO and Glutathione in Normal and Diethyl Maleate-Treated Mouse Brain

As to the subcelluar distribution of ^{99m}Tc-*meso*-HMPAO in normal brain, major portions of radioactivity were found in the mitochondrial (49.0%) and cytosolic (33.0%) fraction, and the levels in the nuclear and microsomal fraction were 5.0 and 13.1%, respectively (Fig. 1). The GSH content was high in the cytosolic fraction (63.2%) and in the mitochondrial, microsomal and nuclear fractions was 30.6%, 4.7% and 1.5%, respectively (Fig. 2). The subcellular distribution of ^{99m}Tc-*d,l*-HMPAO differed slightly from that of *meso*-isomer. The relative radioactivity in the microsomal fraction was higher than that in *meso*-isomer and nearly the same as that in the cytosolic fraction (Fig. 1).

The enzyme assay indicated that almost all enzymatic activity

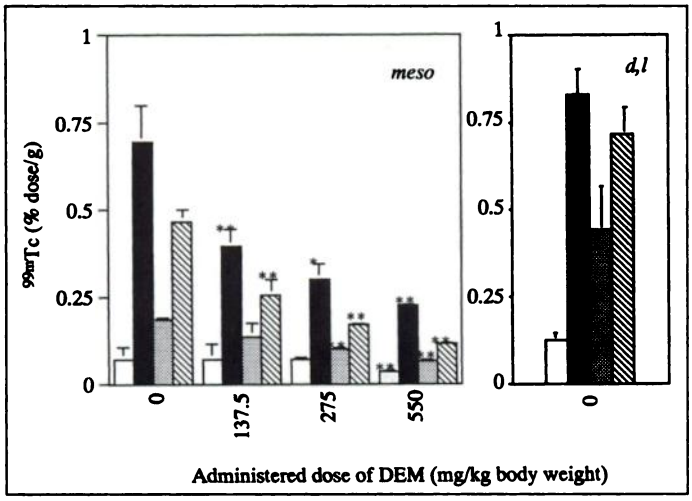

FIGURE 1. Effect of DEM on ^{99m}Tc radioactivity in nuclear (□), mitochondrial (■), microsomal (▨) and cytosolic (▧) fractions. *p<0.05; **p<0.01: significantly different from control level (no DEM).

of cytochrome *c* oxidase was found in the mitochondrial fraction (Fig. 3). Lactate dehydrogenase enzyme activity was found mainly in the cytosolic fraction, but it was also distributed in the mitochondrial and the microsomal fractions (Fig. 3).

Levels of radioactivity in mitochondrial, cytosolic, microsomal and nuclear fractions were decreased in a dose-dependent manner by DEM treatment, which depletes GSH through the glutathione S-transferase. Depletion of radioactivity by DEM treatment was marked in cytosolic and mitochondrial fractions. The DEM treatment (550 mg/kg) reduced the radioactivity to 24.7%, 32.2%, 35.1% and 49.2% of the control level in the cytosolic, mitochondrial, microsomal and nuclear fraction, respectively (Fig. 1). The GSH content in mitochondrial and cytosolic fractions also decreased in a dose-dependent manner on DEM treatment. The DEM treatment (550 mg/kg) reduced the GSH content to 30.0%, 29.3%, 58.0% and 47.0% of the control level in the cytosolic, mitochondrial, microsomal and nuclear fraction, respectively (Fig. 2).

Levels of ^{99m}Tc-*meso*-HMPAO radioactivity and GSH content in subcellular fractions obtained from 18 animals (control, n = 5; DEM treated (137.5 mg/kg), n = 4; (275 mg/kg), n = 4 and (550 mg/kg), n = 5), are plotted in Figure 4. A good correlation was found between the level of ^{99m}Tc-*meso*-HMPAO radioactivity and GSH content in mitochondrial, cytosolic and nuclear fractions, but not in the microsomal fraction: the correlation coefficient (*r*) was 0.81, 0.83, 0.78 and 0.09, respectively. However, the relationship between ^{99m}Tc-*meso*-HMPAO radioactivity and GSH content was not necessarily linear.

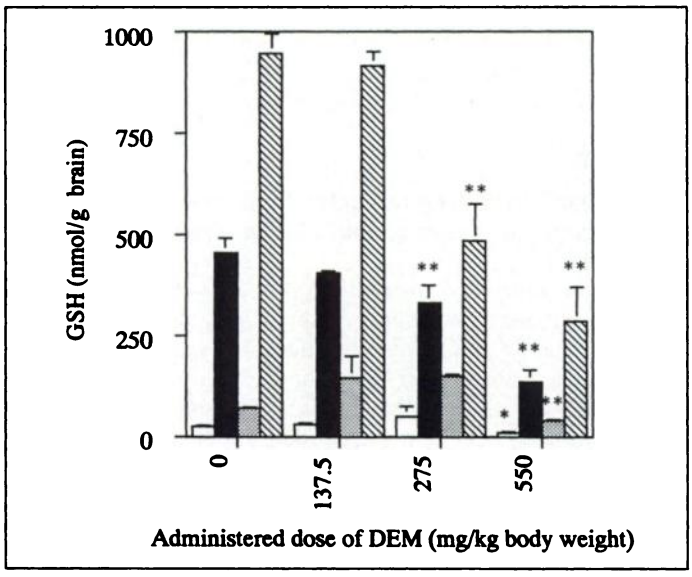

FIGURE 2. Effect of DEM on GSH content in nuclear (□), mitochondrial (■), microsomal (▨) and cytosolic (▧). *p<0.05; **p<0.01: significantly different from control level (no DEM).

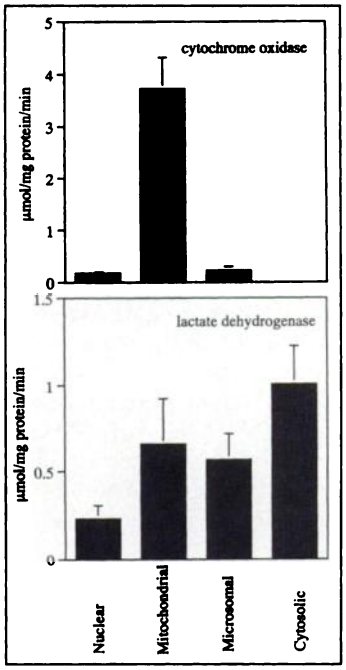

FIGURE 3. Subcellular distribution of cytochrome oxidase and lactate dehydrogenase enzyme activity. Each value is expressed as μmol/mg protein/min.

Calculated concentrations of ^{99m}Tc-*meso*-HMPAO radioactivity and GSH were 0.0156 ± 0.0005% dose/μl and 10.5 ± 1.3 nmol/μl for mitochondrial matrix and 0.00338 ± 0.00009% dose/μl and 6.87 ± 0.43 nmol/μl for cytoplasm.

Release of Technetium-99m Radioactivity, Glutathione and Citrate Synthase Enzyme from the Mitochondrial Fraction by Membrane Solubilizers

About 75.7% of ^{99m}Tc-*meso*-HMPAO radioactivity was released from the mitochondrial fraction by the treatment of Triton X-100 with sonication, while only 14.3% was released by digitonin treatment. The release of citrate synthase, a marker enzyme of mitochondrial matrix, and GSH from the mitochondrial fraction was 81.4 and 80.5% by Triton X-100 with sonication treatment and 5.3 and 13.4% by digitonin treatment, respectively. The effect of those treatments showed a good correlation among the release of ^{99m}Tc-*meso*-HMPAO radioactivity, citrate synthase and GSH from mitochondria (Fig. 5).

DISCUSSION

In terms of the distribution of ^{99m}Tc-*meso*-HMPAO radioactivity, the subcellular fractions ranked as follows: mitochondrial > cytosolic > microsomal ≫ nuclear (Fig. 1). The GSH content was cytosolic > mitochondrial ≫ microsomal > nuclear fraction, which did not necessarily agree with that of ^{99m}Tc radioactivity (Fig. 2). We evaluated ^{99m}Tc-*meso*-HMPAO radioactivity and GSH concentration by assuming the water content in their spaces, based on the theory proposed by Soboll et al. (*14*), to be 0.0156 ± 0.0005% dose/μl and 10.5 ± 1.3 nmol/μl for mitochondrial matrix, and 0.00338 ± 0.00009% dose/μl and 6.87 ± 0.43 nmol/μl for cytoplasm. The mitochondrial matrix/cytoplasm ratio of ^{99m}Tc-*meso*-HMPAO radioactivity and GSH concentration were 4.62 and 1.53, respectively. The GSH concentration in mitochondrial matrix

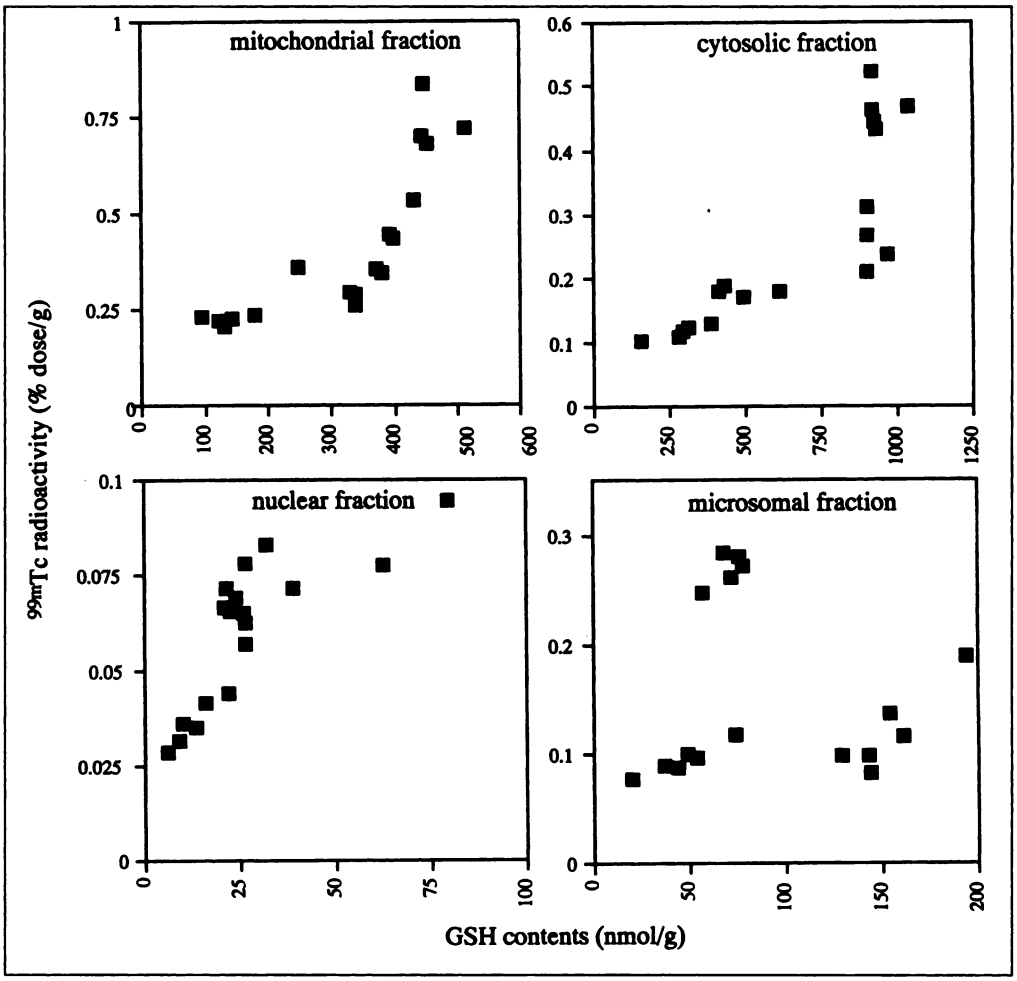

FIGURE 4. Relationship between ^{99m}Tc radioactivity (ordinate) and GSH content (abscissa) in mitochondrial, cytosolic, nuclear and microsomal fractions.

was slightly higher than that in the cytosolic space. This is in good agreement with previous reports that the GSH ratio of mitochondrial matrix/cytoplasm was 1.34 (*8*) and 1.43 (*9*). Since there was no information about the water content in microsomal or nuclear spaces, concentrations of ^{99m}Tc-*meso*-HMPAO radioactivity and GSH in those spaces were not calculated. Although the water content used in the estimation was derived from cultured hepatocytes (*8,9,14*), and may not be applicable to the brain, the present results suggest that more than half of ^{99m}Tc-*meso*-HMPAO uptake in the brain is retained in the mitochondrial fraction.

The difference between ^{99m}Tc-*meso*- and *d,l*-HMPAO in subcellular distributions is shown in Figure 1. The relative percentage of ^{99m}Tc-*d,l*-HMPAO radioactivity in cytosolic and microsomal fractions was higher than for the *meso*-isomer. In a previous study, we showed that the *meso*-isomer was distributed in a GSH-dependent manner, whereas *d,l*-isomar was not. This is because the rate constant for reaction between GSH and the *meso*- isomer is much smaller than that for reaction between GSH and the *d,l*-isomer (*1*). To reach the mitochondrial matrix, ^{99m}Tc-HMPAO travels across three lipid membranes (plasma membrane, mitochondrial inner- and outer-membranes). We speculate that much more ^{99m}Tc-*d,l*-HMPAO radioactivity is trapped in the cytosolic space before the molecule reaches the mitochondria because of the faster conversion to hydrophilic complex by GSH than ^{99m}Tc-*meso*-HMPAO. The relative percentages of ^{99m}Tc-*d,l*-HMPAO radioactivity retained in the cytosolic and microsomal fractions, which contained lower levels of GSH, were higher than those of *meso*-isomer (Fig. 1).

The effect of DEM on the subcellular distribution of ^{99m}Tc-*meso*-HMPAO and GSH was studied (Figs. 1 and 2). The uptake of ^{99m}Tc-*meso*-HMPAO and GSH content, were reduced in a dose-dependent manner by DEM in both the mitochondrial and cytosolic fraction.

To confirm the separation of subcellular components, marker enzyme activity was measured. Cytochrome *c* oxidase enzyme, a marker of mitochondria (*11*), was found almost exclusively in the mitochondria in this study. Lactate dehydrogenase, a marker enzyme of cytoplasm (*11*), distributed preferentially in the cytosolic fraction, while it was also found in the mitochondrial and the microsomal fractions. This extra cytoplasmic distribution of lactate dehydrogenase is considered to be due to contamination by synaptosomes in these fractions.

Digitonin reacts specifically with cholesterol (*16*). Since the plasma membrane contains more cholesterol than the mitochondrial membrane, digitonin at low concentration disrupts the plasma membrane without destroying the mitochondrial membrane (*16*). Since the synaptosomal membrane is made up of neuronal plasma membrane, it is also damaged by low concentrations of digitonin (0.5 mg/ml) (*15*). On the other hand, neuronal mitochondrial membrane resists digitonin and is only destroyed by treatment with Triton X-100 and sonication (*17*). In this study, we treated the pooled mitochondrial fraction isolated from ^{99m}Tc-*meso*-HMPAO-administrated mice brain with these two detergents to estimate the uptake in the mitochondrial fraction. About 75.7% of ^{99m}Tc-*meso*-HMPAO radioactivity in the mitochondrial fraction was released by the treatment with Triton X-100 and sonication, while the figure was only 14.3% for digitonin treatment. A good correlation was found among releases of ^{99m}Tc-*meso*-HMPAO radioactivity

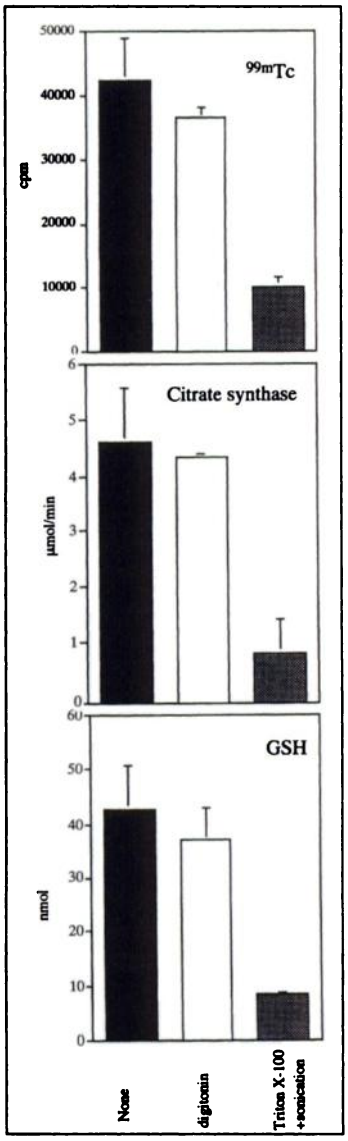

FIGURE 5. Reduction of ^{99m}Tc radioactivity, citrate synthase enzyme and GSH content from mitochondrial fraction by digitonin or Triton X-100 + sonication treatment.

and citrate synthase, a marker enzyme of mitochondrial matrix (*19*) and GSH from mitochondria (Fig. 5). These results indicate that almost all ^{99m}Tc radioactivity in the mitochondrial fraction existed within mitochondria.

Technetium-99m-*d,l*-HMPAO has been applied to labeling of liposomes that are a potential tumor imaging agent (*19*). When liposomes containing GSH in aqueous phase are treated with ^{99m}Tc-*d,l*-HMPAO, the lipophilic radiotracer diffuses across the lipid membrane, is converted into a hydrophilic form by GSH and accumulates within the liposomes. Localization of ^{99m}Tc radioactivity in the liposomal aqueous phase was confirmed by water-octanol extraction (*19*). As a mitochondrion has the structure of a lipid bilamella, it is regarded as a kind of liposome. The results of this study suggested that mitochondria trapped ^{99m}Tc-*meso*-HMPAO radioactivity within their aqueous phase just like liposomes labeled with ^{99m}Tc-*d,l*-HMPAO.

A good correlation was found between radioactivity of ^{99m}Tc-*meso*-HMPAO and GSH content in mitochondrial, cytosolic and nuclear fractions, respectively (Fig. 3). However, the regression line between ^{99m}Tc radioactivity and GSH content in the cytosolic fraction was different from that in the mitochondrial or nuclear fractions. Mitochondria accumulated about three times as much ^{99m}Tc as cytosol for the same GSH content. There are two possible explanations for this, first, GSH concentration rather than content is a significant factor in the trapping of ^{99m}Tc-HMPAO radioactivity in closed intracellular spaces. We calculated concentrations of GSH in mitochondrial matrix and cytoplasm. The mitochondrial fraction contained 1.53 times as much GSH concentration as the cytosolic fraction. The mitochondrial matrix/cytoplasm ratios of GSH were reported as 1.34 (*8*) and 1.43 (*9*) using cultured hepatocytes. Second, although homogenization and centrifugation were done at 4°C or below within a minimum time period, a nonenzymatic reaction may occur for the conversion of ^{99m}Tc-HMPAO to hydrophilic complex (*2*). Therefore, the remaining intact ^{99m}Tc-*meso*-HMPAO might have redistributed into mitochondria from the cytosolic phase in homogenate.

Mitochondria is a major source of reactive oxygen species (ROS) (*20*). Dysfunction of the mitochondrial electron transport system and imbalance among mitochondrial electron transfer carriers causes an increased level of ROS and may lead to cell death (*21,22*). Leakage of ROS from mitochondria is considered to determine the life span in animal species (*23*). GSH is a main antioxidant in the brain and contributes to the clearance of H_2O_2 through glutathione peroxidase (*20*). Reduction of mitochondrial GSH content was reported in aged animal brain and Parkinson's disease brain (*20,22*). The reduction of mitochondrial GSH content may cause increasing leakage of ROS from the mitochondria (*22*). Reduction of GSH in mitochondria is critical to cell death, while that in cytoplasm is not (*6,24*). These observations indicate that determination of GSH content in cerebral mitochondria may be valuable for assessment of the oxidative stress in brain. In this study, the mitochondria are a major subcellular fraction for the uptake of ^{99m}Tc-*meso*-HMPAO by the brain, and a good correlation was found between radioactivity of ^{99m}Tc-*meso*-HMPAO and GSH content in the mitochondrial fraction. Technetium-99m-*meso*-HMPAO might be used as an indicator to assess the mitochondrial GSH and the oxidative stress in the brain.

CONCLUSION

Mitochondria are a major subcellular fraction for the uptake of ^{99m}Tc-*meso*-HMPAO by the brain, and that GSH in mitochondria contributes to the accumulation of ^{99m}Tc-*meso*-HMPAO. Technetium-99m-*meso*-HMPAO might be used as an indicator to assess the mitochondrial GSH and the oxidative stress in the brain.

ACKNOWLEDGMENTS

We thank Dr. J.D. Kelly, Amersham International, United Kingdom, for the kind gift of *meso*-HMPAO. This work was supported by Grant-in-Aid for Scientific Research (C) from the Japanese Ministry of Education, Science, Sports and Culture.

REFERENCES

1. Sasaki T, Toyama H, Oda K, et al. Assessment of antioxidative ability in brain: technetium-99m meso-hexamethyl propyleneamine oxime as an imaging agent for glutathione localization. *J Nucl Med* 1996;37:1698–1701.
2. Sasaki T, Senda M. Technetium-99m *meso*-hexamethyl propyleneamine oxime as a potential agent for imaging cerebral glutathione content. *J Nucl Med* 1997;38:1125–1129.
3. Ballinger JR, Reid RH, Gulenchyn KY. Technetium-99m HMPAO stereoisomers: differences in interaction with glutathione. *J Nucl Med* 1988;29:1998–2000.
4. Neirinckx RD, Burke JF, Harrison RC, et al. The retention mechanism of technetium-99m-HMPAO: intracellular reaction with glutathione. *J Cereb Blood Flow Metab* 1988;8:S4–S12.
5. Fujibayashi Y, Taniguchi H, Waki A, et al. Intracellular metabolism of ^{99m}Tc-*d,l*-HMPAO in vitro: a basic approach for understanding the hyperfixation mechanism in damaged brain. *Nucl Med Biol* 1998;25:375–378.
6. Meister A. Mitochondrial changes associated with glutathione deficiency. *Biochim Biophys Acta* 1995;1271:35–42.
7. Garcia-Ruiz C, Morales A, Colell A, et al. Evidence that the rat hepatic mitochondrial carrier is distinct from the sinusoidal and canalicular transporters for reduced glutathione. Expression studies in Xenopus laevis oocytes. *J Biol Chem* 1995;270:15946–15949.

8. Wahllander A, Soboll S, Sies H. Hepatic mitochondrial and cytosolic glutathione content and the subcellular distribution of GSH-S-transferases. *FEBS Lett* 1979;97: 138–140.
9. Elbers R, Heldt HW, Schmucker P, et al. Measurement of the ATP/ADP ratio in mitochondria and in the extramitochondrial compartment by fractionation of freeze-stopped liver tissue in non-aqueous media. *Hoppe-Seyler's Z Physiol Chem* 1974;355: 378–393.
10. De Robertis E, Pellegrino De Iraldi A, Rodriguez De Lores Arnaiz G, et al. Cholinergic and non-cholinergic nerve endoings in rat brain-I. *J Neurochem* 1962;9:23–35.
11. Sims NR. Rapid isolation of metabolically active mitochondria from rat brain and subregions using Percoll density gradient centrifugation. *J Neurochem* 1990;55:698-707.
12. Dunkley PR, Jarvie PE, Heath JW, et al. A rapid method for isolation of synaptosomes on Percoll gradients. *Brain Res* 1986;372:11–129.
13. Lowry OH, Rosebrough NJ, Farr AL, Randall RJ. Protein measurements with the Folin phenol reagent. *J Biol Chem* 1951;193:265–275.
14. Soboll S, Scholz R, Heldt HW. Subcellular metabolite concentrations dependence of mitochondrial and cytosolic ATP systems on the metabolic state of perfused rat liver. *Eur J Biochem* 1978;87:377–390.
15. Booth RF, Clark JB. A method for the rapid separation of soluble and particulate components of rat brain synaptosomes. *FEBS Lett* 1979;107:387–392.
16. Meredith MJ, Reed DJ. Status of the mitochondrial pool of glutathione in the isolated hepatocyte. *J Biol Chem* 1982;257:3747–3753.
17. Bonnefoi MS. Mitochondrial glutathione and methyl iodide-induced neurotoxicity in primary neural cell cultures. *Neurotoxicol* 1992;13:401–412.
18. Srere PA. Citrate synthase. *Methods Enzymol* 1969;13:3–11.
19. Ogihara-Umeda I, Sasaki T, Kojima S, et al. Optimal radiolabeled liposomes for tumor imaging. *J Nucl Med* 1996;37:326–332.
20. Benzi G, Moretti A. Age- and peroxidative stress-related modifications of the cerebral enzymatic activities linked to mitochondria and the glutathione system. *Free Radic Biol Med* 1995;19:77–101.
21. Cortopassi G, Wang E. Modelling the effects of age-related mtDNA mutation accumulation; complex I deficiency, super oxide and cell death. *Biochim Biophys Acta* 1995;1271:171–176.
22. Benzi G, Pastoris O, Marzatico F, et al. The mitochondrial electron transfer alteration as a factor involved in the brain aging. *Neurobiol Aging* 1992;13:361–368.
23. Barja G, Cadenas S, Rojas C, et al. Low mitochondrial free radical production per unit O_2 consumption can explain the stimultaneous presence of high longevity and high aerobic metabolic rate in birds. *Free Radic Res* 1994;21:317–328.
24. Meredith MJ, Reed DJ. Depletion in vitro of mitochondrial glutathione in rat hepatocytes and enhancement of lipid reroxidation by adriamycin and 1,3-bis(2-chloroethyl)-1-nitorosourea (BCNU). *Biochem Pharmacol* 1983;32:1383–1388.

Multiple Line Source Array for SPECT Transmission Scans: Simulation, Phantom and Patient Studies

A. Celler, A. Sitek, E. Stoub, P. Hawman, R. Harrop and D. Lyster
Vancouver Hospital and Health Sciences Centre, and University of British Columbia, Vancouver, British Columbia, Canada; and Siemens Medical Systems, Inc., Hoffman Estates, Illinois

Accurate attenuation and scatter corrections in quantitative SPECT studies require attenuation maps of the density distribution in the scanned object. These can be obtained from simultaneous emission/transmission scans. **Methods:** A new method has been developed using a multiple line source array (MLA) for transmission scans, and its performance has been investigated using computer simulations and experimental data. The activity in the central lines of the MLA was higher than at the edges of the system, so that more transmission photons would be directed toward the thicker parts of the human body. A series of transmission-only and simultaneous emission/transmission studies were performed for different phantom configurations and human subjects. Attenuation maps were generated and used in reconstruction of attenuation-corrected emission images. **Results:** The μ coefficients for attenuation maps obtained using the MLA system and simulated and experimental data display no artifacts and are qualitatively and quantitatively correct. For phantoms, the agreement between the measured and the true value of μ for water was found to be better than 4%. The attenuation-corrected emission images for the phantom studies demonstrate that the activity in the heart can be accurately reconstructed. A significant qualitative improvement was also obtained when the attenuation correction was used on patient data. **Conclusion:** Our results indicate that the MLA transmission source can be used in simultaneous transmission/emission imaging to generate accurate attenuation maps. These maps allow for performing an object-specific, attenuation correction of the emission images.

Key Words: SPECT; attenuation correction; transmission source

J Nucl Med 1998; 39:2183–2189

Received Nov. 3, 1997; revision accepted Apr. 30, 1998.

For correspondence or reprints contact: A. Celler, PhD, FCCPM, Division of Nuclear Medicine, Vancouver Hospital and Health Sciences Centre, 855 West 12th Ave., Vancouver, British Columbia, V5Z 1M9, Canada.

Accurate methods for attenuation correction, based on experimental attenuation maps, are considered essential for data quantitation in SPECT imaging (*1–3*). Such maps allow for proper account to be made of the nonuniform distribution of the attenuating medium and, potentially, for density-dependent estimation of the scatter distribution (*4*).

In general, transmission source configurations can be classified into two groups, depending on the detector collimation. The first group uses standard, parallel-hole detector collimation, and transmission is provided either by a sheet source used without (*5*) or with (*6,7*) a collimator or a scanning line source, mostly used with dual-head 90° cameras (*8*). The second group, mostly used with triple-head cameras, requires special converging detector collimators. In this group, a single collimated line source is placed in the focal position of a symmetric (*9*) or an asymmetric (*10,11*) fanbeam detector collimator.

All of these approaches, however, have disadvantages. An uncollimated sheet source generates a map of broad-beam attenuation coefficients, whereas use of a collimator in front of such a source results in substantially increased activity and weight. The scanning line source technique requires complicated electronic equipment to control its run-time operations. Also, because the same activity is used to scan the whole range of tissue thicknesses, the source must be quite strong to produce sufficient counts for large patients. This causes substantial dead time losses can occur at the edges of the detector, where the source illuminates only the periphery of the body and attenuation is low or null. Truncation artifacts, which are inherent in the symmetric fanbeam geometry, have been eliminated with the asymmetric fanbeams at a cost of using a full 360° camera rotation.

A transmission source consisting of four-fixed position collimated line sources was proposed by Larsson et al. (*12*).